

Reaction kinetics of dual setting α -tricalcium phosphate cements

Katrin Hurle¹ · Theresa Christel² · Uwe Gbureck² · Claus Moseke² · Juergen Neubauer¹ · Friedlinde Goetz-Neunhoffer¹

Received: 17 June 2015 / Accepted: 28 October 2015 / Published online: 26 November 2015
© Springer Science+Business Media New York 2015

Abstract Addition of ductile polymers to calcium-deficient hydroxyapatite (CDHA)—forming bone cements based on α -tricalcium phosphate (α -TCP) is a promising approach to improve the mechanical performance of α -TCP cements and extend their application to load-bearing defects, which is also impeded by the brittleness of the hardened cement. One suitable polymer is poly-(2-hydroxyethylmethacrylate) (p-HEMA), which forms during cement setting by radical polymerisation of the monomer. In this study the hydration kinetics and the mechanical performance of α -TCP cements modified with addition of different HEMA concentrations (0–50 wt% in the cement liquid) was investigated by quantitative in situ XRD and four-point bending tests. Morphology of CDHA crystals was monitored by scanning electron microscopy. The hydration of α -TCP to CDHA was increasingly impeded and the visible crystal size of CDHA increasingly reduced with increasing HEMA concentration. Modification of the cements by adding 50 wt% HEMA to the cement liquid changed the brittle performance of the hardened cement to a pseudoplastic behaviour, reduced the flexural modulus and increased the work of fracture, while lower HEMA concentrations had no significant effect on these parameters. In such a composite, the extent of CDHA formation was considerably reduced (34.0 ± 1.8 wt% CDHA with

50 % HEMA compared to 54.1 ± 2.4 wt% CDHA in the reference formed after 48 h), while the general reaction kinetics were not changed. In conclusion, while the extent of CDHA formation was decreased, the mechanical properties were noticeably improved by addition of HEMA. Hence, α -TCP/HEMA composites might be suitable for application in some load-bearing defects and have adequate properties for mechanical treatment after implantation, like insertion of screws.

1 Introduction

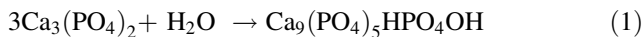
Mineral bone cements based on calcium phosphate chemistry offer the advantages of a free moldability with a high cytocompatibility and a good mechanical stability after setting [1]. Although they are comparatively strong compared to trabecular bone with compressive strength of up to 80 MPa [2], they suffer from the brittle nature of ceramics and are hence only indicated for non-load bearing bone defects. Reinforcement strategies of CPC to reduce their brittleness are predominantly focused on the addition of fibers, which can bridge cracks under mechanical loading [3], or the modification with a ductile polymeric phase added to the cement powder or liquid prior to setting. The latter approach has been performed by using either natural polymers such as collagen [4, 5] or chitosan [6, 7], or by simultaneously cross-linking water soluble monomers during cement setting [8–10]. Previously used monomers were either acrylamide [8, 9], 2-hydroxyethylmethacrylate (HEMA) [11] or a methacrylate modified dextran [10]. This dual setting concept has been demonstrated to both increase cement strength and reduce cement brittleness due to an increased work of fracture [10, 11]. Most of these investigations were performed for cements based on the

✉ Katrin Hurle
katrin.hurle@fau.de

¹ GeoZentrum Nordbayern – Mineralogy, Friedrich-Alexander-University of Erlangen-Nuremberg, Schlossgarten 5a, 91054 Erlangen, Germany

² Department for Functional Materials in Medicine and Dentistry, University of Würzburg, Pleicherwall 2, 97070 Würzburg, Germany

reaction of α -tricalcium phosphate (α -TCP) to calcium deficient hydroxyapatite (CDHA) [8, 9, 11], with a clear focus on the mechanical cement properties rather than on analysing the mutual influence of inorganic cement setting and organic polymerisation reaction. Both reactions require an aqueous environment and compete for the limited amount of water present in the cement paste. An aqueous phase is necessary for the inorganic cement setting reaction to dissolve cement raw materials and precipitate the final setting product, with only a small amount of water being incorporated into the setting product according to:



Setting of α -TCP cements is a comparatively slow reaction, e.g. it was shown by Ginebra et al. [12] that only 80 % of α -TCP has been reacted after 24 h, despite of a relatively small α -TCP particle size of 6.3 μm . In contrast, the polymerisation reaction of monomers is fast (mostly finished after a maximum of 30 min) and physically binds a considerable amount of water in the formed hydrogel. It is obvious that the reduced amount of free water will result in retarding the inorganic cement setting and indeed, Christel et al. found a lower degree of cement conversion for dual setting α -TCP/HEMA cements (80–85 %) compared to the polymer free reference (96 %) after 7 days setting [11]. Since the degree of cement conversion is linearly related to cement strength [13] and the strength development in biocements is a crucial parameter for an application in load bearing defects, a profound knowledge about the setting kinetics and the corresponding mechanical properties of such cements is pivotal. In addition, an early strength development of the cement immediately after implementation will avoid the formation of cracks within the cement structure (e.g. caused by surgical manipulations at the implant site or by movement of the patient) and it might also help to apply further surgical techniques such as drilling for screw fixation. This implies the necessity of time-resolved studies of the setting reaction. In-situ XRD measurements offer a good opportunity to study the hydration reaction in the setting cement from the first minutes after implementation. Furthermore, if the CDHA formation rate and development of CDHA crystal sizes can be correlated with the time-resolved development of mechanical properties, a more detailed basic understanding of the setting mechanism of cements with and without HEMA modification can be achieved to further optimise cement formulations.

Therefore, this study aims to investigate the setting kinetics of dual setting calcium phosphate cements in more detail. Cements were made from α -TCP powder with HEMA as water soluble monomer. The setting reaction was followed by X-ray diffraction analysis over a course of 2 days, whereas the amount of crystalline α -TCP and of the

setting product CDHA was time-dependently and quantitatively calculated by Rietveld refinement analysis and subsequent application of the G-factor method, an external standard method which facilitates determination of absolute phase quantities [14]. The composites were further characterised with regard to their four-point bending strength after various time intervals to correlate strength development with the setting reaction.

2 Materials and methods

2.1 Sample preparation

Cements in this study were composed of phase pure α -tricalcium phosphate (α -TCP, α - $\text{Ca}_3(\text{PO}_4)_2$), which was synthesized by a solid state reaction (1400 °C, 5 h) from a mixture of monetite (CaHPO_4 ; Mallinckrodt Baker, Griesham, Germany) and calcium carbonate (CaCO_3 ; Merck, Darmstadt, Germany). The sintered cake was quenched in air to room temperature, crushed with mortar and pestle to a particle size <355 μm and finally ground in a planetary ball mill (PM400 Retsch, Germany) for 4 h. The particle size distribution of the α -TCP raw powder was analyzed before and after milling via laser particle size analyzer L300 (Horiba, Kyoto, Japan). The particles were suspended in 200 ml isopropanol for at least 15 min applying ultrasound. Their size d_{50} was found to be 21.09 μm before grinding and 4.62 μm afterwards.

Cement liquids were either a 2.5 % Na_2HPO_4 solution (reference) or an aqueous solution consisting of 2.5 % Na_2HPO_4 (Merck, Darmstadt, Germany) and either 10, 25 wt% respectively 50 wt% 2-hydroxyethylmethacrylate (HEMA, Merck, Darmstadt, Germany). To initiate polymerisation, the cement powder was supplemented with 0.5 wt% ammonium persulfate (APS, Sigma Aldrich Chemie GmbH, Steinheim, Germany), and 0.25 wt% N,N,N',N' -tetramethylethylenediamine (TEMED, Sigma Aldrich Chemie GmbH, Steinheim, Germany) was added to the cement liquid.

2.2 Mechanical tests

For the mechanical tests, cement pastes were formed by mixing the ground α -TCP powder with cement liquid on a glass slab for 30 s at a liquid to powder ratio (LPR) of 0.33 ml/g. Cement pastes were transformed into silicon rubber moulds to prepare samples for four-point bending strength ($3 \times 4 \times 45 \text{ mm}$) testing and allowed to set at 37 °C for time periods of 2 h, 4 h, 6 h, 12 h, 24 h, 2 days and 7 days in a water bath. Following this, wet samples ($n = 9$ per condition) were tested for four-point bending using a static mechanical testing machine Zwick Z010

(Zwick, Ulm, Germany) with a 2.5 kN load cell and a crosshead speed of 1 mm/min. Analysis of variance was examined by means of the excel sheet inerSTAT-a (M.H.Vargas, Instituto Nacional de Enfermedades, Mexiko).

2.3 SEM analysis

After bending, the samples were dried at 40 °C (reference) or freeze-dried (samples with HEMA). A 20,000-fold magnification of the fracture surfaces was examined via scanning electron microscope Crossbeam 340 (SEM, Zeiss, Oberkochen, Germany) with an acceleration voltage of 2.0 kV and the detection of secondary electrons. Before the samples were coated with a 4 nm layer of gold.

2.4 Quantitative XRD measurements

The quantitative phase composition of the α -TCP powder used in this study was determined by powder XRD. The powder was prepared by front-loading method, three independently prepared powder samples were measured. In-situ XRD was performed with samples containing 0 (reference) respectively 50 wt% HEMA (HEMA_50) in the cement liquid to determine the development of the quantitative phase content during hydration. The cement pastes for the quantitative in situ XRD measurements were prepared by adding the cement liquid to the powder at a LPR of 0.33 ml/g and stirring it for 1 min with a plastic spatula in a plastic container. The as-prepared cement pastes were then filled in a special sample holder and covered with a Kapton polyimide film (Chemplex Industries, Cat. No. 440) to reduce water evaporation during measurement. The temperature of the sample holder was adjusted at 37 °C with a Peltier stage.

All XRD measurements were performed at a D8 Advance with DaVinci design diffractometer (Bruker AXS, Karlsruhe). The following parameters were applied for the powder measurements: range 10°–60° 2 θ ; step size 0.011° 2 θ ; integration time 0.5 s; radiation: copper K α ; generator settings: 40 mA, 40 kV; divergence slit: 0.3°. For the in situ XRD measurements, the range was reduced to 10°–35° 2 θ and the integration time to 0.35 s. 198 ranges were recorded, the measurement time for one range was nearly 15 min, resulting in an overall measurement time of 48 h. In situ XRD was reproduced three times for the reference and five times for HEMA_50, as the results were less reproducible here.

Rietveld refinement with subsequent G-factor quantification was applied to obtain the absolute quantities of the crystalline phases α -TCP and CDHA. For the powder sample the G-factor method was mainly applied to determine the quantity of amorphous TCP (ATCP) after

intensive milling of the α -TCP powder. Rietveld refinement was accomplished with the software TOPAS 4.2 (Bruker AXS, Karlsruhe). The α -TCP structure ICSD# 923 [15] and the HAp structure ICSD# 26204 [16] were applied together with a first order Chebychev background. The ATCP content of the samples, the signal of the Kapton film and the water were each modelled by a separate peak phase in TOPAS. The anisotropic crystallinity of CDHA was modelled by a triaxial ellipsoid model (Fig. 1) [17], which proved to result in the best fits compared to other models available for hexagonal crystallites. Due to requirements of the hexagonal symmetry, rx and ry were set to the same value. rx corresponds to the direction of the crystallographic a axis and rz to the direction of the crystallographic c-axis. For the in situ XRD, the refinement was performed for each single diffractogram to determine the quantitative phase content at each time.

The G-factor method is an external standard method which allows determination of absolute phase quantities [14]. In this study, a quartzite was used as external standard. From this standard, the device-specific G-factor can be calculated according to (2).

$$G = S_q \frac{\rho_q V_q^2 \mu_q^*}{c_q} \quad (2)$$

Here S_q is the Rietveld scale factor, ρ_q the density, V_q the unit-cell volume and c_q the weight fraction of quartz. μ_q^* is the mass attenuation coefficient (MAC) of the quartzite [14]. The quartzite sample itself was calibrated with silicon powder, which is assumed to be 100 % crystalline silicon. The absolute content of any crystalline phase j in the sample investigated can then be determined from the Rietveld scale factors using (3):

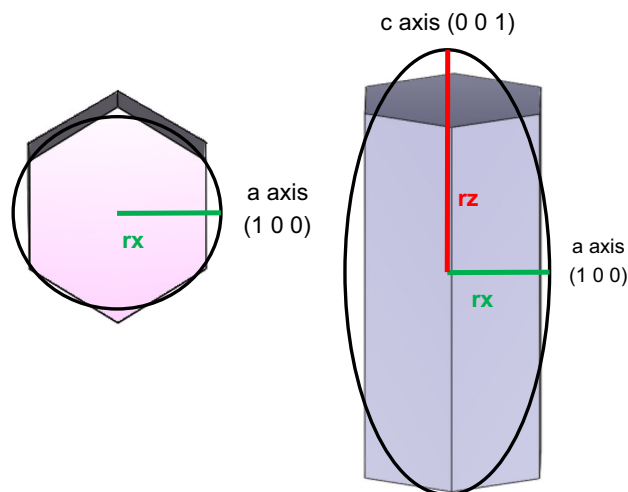


Fig. 1 Model ellipsoid for refinement of the anisotropic crystallite size of CDHA according to [17]. The model for the hexagonal CDHA crystallite in the graphic was created with VESTA [23]

$$c_j = S_j \frac{\rho_j V_j^2 I_{sample}^*}{G} \quad (3)$$

The MAC values of the elements, which were used to calculate μ^* of the samples, were taken from the International Tables for Crystallography [18]. For calculating the MAC of the cement pastes, all components, including the starters APS and TEMED, were taken into account.

In order to determine the water loss during hydration, which is important for calculation of the MAC, the samples' water content directly after the in situ measurements was determined by drying the samples at 80 °C in an oven and measuring the weight loss, which is equivalent to the water content at the end of the measurement. Assuming a constant evaporation rate during the measurement, the water content of the samples and accordingly the MAC could then be calculated for each time. Average weight loss was 18.6 ± 1.3 wt% in the reference and 9.6 ± 0.2 wt% in HEMA_50, which means that the water content of the samples was reduced from 24.4 to 7.8 ± 1.5 wt% in the reference and from 12.8 to 3.5 ± 0.4 wt% in HEMA_50 cement.

The water loss during hydration, which is inevitable in the experimental setup of the in situ XRD, considerably affects the hydration reaction. Hence it was necessary to correct the quantities directly received from the in situ measurements to obtain the development of the quantitative phase contents, as it would occur without water evaporation. For this purpose, plastic cups were completely filled with the mixed cement pastes, closed with a lid and tightly sealed with Parafilm. These samples were stored for 24 and 48 h in an oven at 37 °C. For HEMA_50 cements, where the effect of water evaporation was more pronounced, further samples were hardened for 6 and 12 h. In order to check if the hydration still proceeds after 48 h, additional samples were stored for 7 days. For each hydration time, the preparation was reproduced three times. The water loss of the samples during storage in the drying oven was checked to control if the aim of eliminating water evaporation could really be achieved. A maximum weight loss of 0.5 wt% was measured for a reference sample after storage over 7 days, which is actually negligible.

After the desired hydration time the storage samples were sawed in the plastic cups using isopropyl alcohol as lubricant and prepared in special sample holders for XRD measurements. In order to achieve comparability with the in situ XRD measurements, these samples were also covered with a Kapton film and measured with the same conditions as the in situ XRD samples. Three ranges of each sample were recorded. The water content of these samples during XRD was determined by drying the sample directly after the measurement and measuring the weight loss.

As for the method described above a separate sample has to be prepared for every desired measurement time, while by in situ XRD data for the whole hydration time can be obtained from one single sample, in situ measurements were still important to obtain general information about the hydration kinetics with sufficient time resolution. This is why a combination of in situ XRD and investigation of selected storage samples was chosen to obtain information about the setting mechanism in an environment without water loss. By comparing the results of both methods, it was shown that the water loss during in situ measurements actually strongly affected the hydration. In the sample HEMA_50, CDHA content after 48 h showed 33.7 ± 2.3 wt% in the storage sample compared to 23.8 ± 1.8 wt% in the in situ sample.

For crystalline α -TCP and CDHA, the ratios of the phase contents in the storage samples to the corresponding quantities in the in situ measurements were calculated and plotted against the hydration time. The quantities were priorly corrected in respect of the water contents of the samples to render them directly comparable and eliminate an apparent increase of phase content that would result from water evaporation, i.e. they were corrected to the quantities which would be measured if no water loss had occurred.

Regression lines were then determined for these values to obtain the ratio for each time (Fig. 2). The quantities directly obtained from in situ XRD were then multiplied

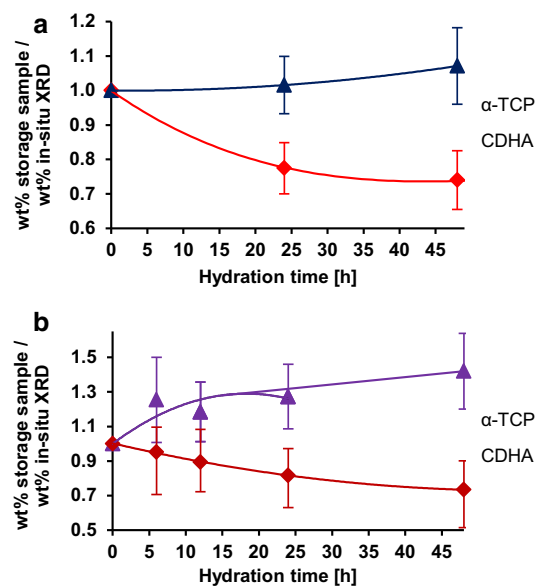


Fig. 2 Regression lines of the ratios wt% (storage sample)/wt% (in situ XRD) for the reference (a) and HEMA_50 (b). The samples were made of α -TCP and a 2.5 % Na_2HPO_4 solution (reference) or of α -TCP and 50 % HEMA solution (HEMA_50) with a LPR of 0.33 ml/g; storage samples were stored in sealed plastic cups at 37 °C in a drying oven

with the corresponding factor to obtain the phase content development without evaporation. From this corrected XRD data, a continuous curve was created with the peak finding and fitting software Fityk [19]. The derivatives of the curves, which describe the speed of dissolution respectively formation, were also calculated by Fityk [19].

Additional storage experiments over 48 h were performed for samples containing 10 respectively 25 wt% HEMA in the cement liquid (HEMA_10 and HEMA_25) to obtain information about the correlation between HEMA content and the extent of the hydration reaction.

3 Results

3.1 Mechanical properties of hardened cement samples

Figure 3 shows the development of the four-point bending strength (Fig. 3a), flexural modulus (Fig. 3b) and work of fracture (Fig. 3c) over a time period of 7 days. In the case of pure α -TCP cement the bending strength increased from initially 0.7 ± 0.3 to 6.4 ± 2.1 MPa after 1 week of setting in water at 37 °C. A significant increase in strength could be seen between 6 and 12 h deposition time. The α -TCP/HEMA composites showed a similar course. However, the bending strength started with even 2.8 ± 0.7 MPa after 2 h and ended with 9.9 ± 2.7 MPa after 7 days. In the first 12 h of the deposition study the composite cements HEMA_50 had a significantly and at most four times higher strength compared to the reference (Fig. 3a). Furthermore, α -TCP samples showed an increase in flexural modulus from 0.2 ± 0.1 to 2.7 ± 0.4 GPa and therefore an increase in brittleness. A significant doubling of the flexural modulus took place between a deposition time of 12 and 24 h. In contrast, the α -TCP/HEMA composites showed a less brittle behaviour, but also took an overall increase from 0.1 to 1.0 ± 0.2 GPa that was significant between 6 and 12 h. Except the 12 h time point, flexural moduli of reference samples were always significantly higher than those of the composite cements, at least twice as high (Fig. 3b). A major difference between pure α -TCP and α -TCP/HEMA cements could be seen concerning the work of fracture. Reference samples only showed marginal values between 0.03 ± 0.02 and 0.3 ± 0.2 Nmm during 7 days of deposition, whereas the work of fracture of HEMA containing cements fluctuated between 4.8 ± 1.6 Nmm (4 h) and 10.5 ± 2.5 Nmm (12 h) (Fig. 3c). Figure 3d illustrates again the differences between reference and HEMA_50 concerning their mechanical behaviour. Force–displacement curves of two chosen time points (6, 12 h) demonstrate the time dependent ceramic-like brittleness of pure CPC, while composite samples with

added polymer rather showed a pseudoplastic behaviour at both time points.

We further analysed the influence of different HEMA concentrations (0, 10, 25 or 50 %) on the mechanical behaviour of composite samples after a defined deposition period of 2 days in water at 37 °C (Fig. 4). No significant differences between samples with different HEMA contents could be seen regarding their four-point bending strength (Fig. 4a). With respect to flexural modulus (Fig. 4b), work of fracture (Fig. 4c) and force–displacement curves (Fig. 4d), the samples HEMA_10 and HEMA_25 behaved similar to the reference cement without polymer. Only the addition of 50 % HEMA into the aqueous solution led to a significant reduction of the flexural modulus, an increase in work of fracture and a pseudoplastic force–displacement diagram, as it was already described above.

3.2 CDHA morphology

The time-dependent development of morphology and size of CDHA crystals is shown without (Fig. 5a–g) and with the addition of HEMA in the aqueous phase of the cement paste (Fig. 5h–n). As for the reference, a mixture of small needle-like crystals with a length of 200 nm and rough grains between 0.5 and 2 μ m can be seen after 2 h of setting. The latter can be considered as unreacted α -TCP powder (Fig. 5a). In the course of time the number of α -TCP grains decreased whereas the surface became homogeneously covered with aggregates of CDHA crystals. Besides, the length of the hydroxyapatite crystals increased from approximately 200 nm (Fig. 5a) to ~ 1 μ m (Fig. 5d–g). In addition, mixtures of particles with different sizes (Fig. 5e, g) and characteristically flower-like aggregates (Fig. 5e) can be seen. After a setting time of 12 h, the hydroxyapatite crystals did not seem to further gain in size. The addition of HEMA to the aqueous phase of the cement paste resulted in an obviously diverse surface morphology. After 2 h of setting, the fracture surface appeared really smooth and was rarely covered with small crystals of 100–200 nm in length that did not stick out of the surface but rather were embedded into it (Fig. 5h). In the next 22 h, the number and size of hydroxyapatite crystals slowly increased to ~ 300 nm (Fig. 5i–l). In contrast to the reference fracture surfaces after 24 h of setting the hydroxyapatite crystals were closely interlaced and homogeneous in size and morphology (Fig. 5h). However, the crystal formation and growth was strongly influenced by the addition of HEMA. After 2 and 7 days of setting, the crystals seemed to be glued by a certain amorphous film (Fig. 5m, n). Figure 6 confirms again that HEMA affects

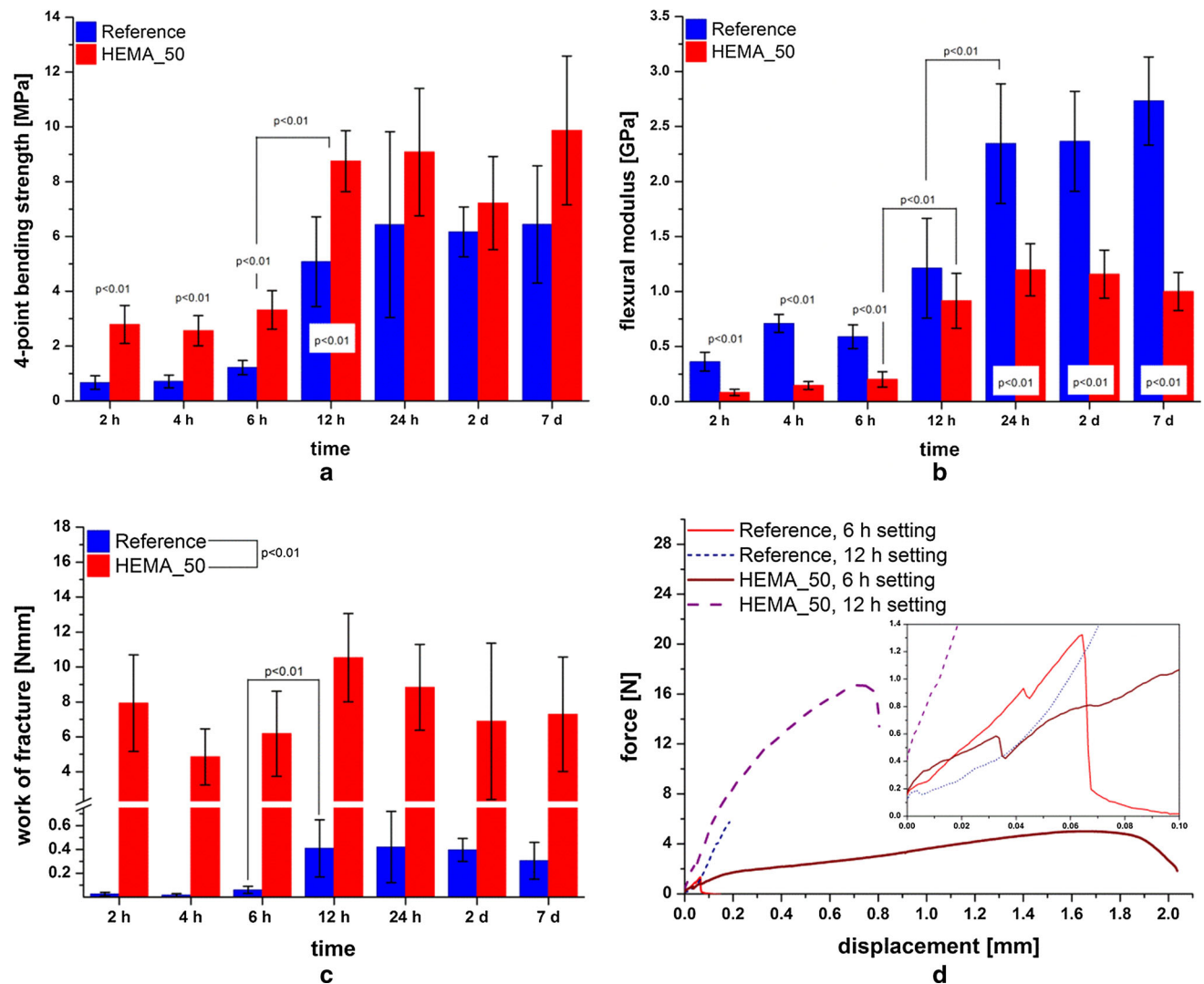


Fig. 3 Four-point-bending strength (a), flexural modulus (b), work of fracture (c) and force displacement curves (d) of samples with a geometry of $3 \times 4 \times 45$ mm. The samples were made of α -TCP and

a 2.5 % Na_2HPO_4 solution (reference) or of α -TCP and 50 % HEMA solution (HEMA_50) with a LPR of 0.33 ml/g and stored for 2 h, 4 h, 6 h, 12 h, 24 h, 2 days or 7 days in water at 37 °C

the crystal size as the addition of 10, 25 or 50 % HEMA in the aqueous phase of the cement paste led to gradually smaller hydroxyapatite crystals (Fig. 6a–d).

3.3 Quantitative XRD of powder samples and hydrating cement pastes

The α -TCP powder used in this study contained 18.4 ± 1 wt% ATCP and 81.6 ± 1.0 wt% crystalline α -TCP. No other secondary phases were detected by XRD. Figure 7 displays the development of the quantitative α -TCP and CDHA content in the reference compared to HEMA_50 (Fig. 7a) together with the corresponding derivatives (Fig. 7b). In both samples, α -TCP dissolution and CDHA formation started immediately at the beginning of the measurement. Maximum dissolution of the crystalline α -TCP

was reached after 1.2 h in the reference and after 1.5 h in HEMA_50 cement. Following the maximum, α -TCP dissolution speed in both samples strongly decreased. It is worth to note that maximum of CDHA formation occurred directly at the start of hydration. The strong initial CDHA formation must have resulted from hydration of the ATCP content, which must have occurred faster than crystalline α -TCP hydration. This was previously observed for partially amorphized α -TCP samples [20].

As can be seen from the heights of the derivatives and especially from the heights of the maxima (Fig. 7b), both α -TCP dissolution and CDHA formation proceeded significantly slower in HEMA_50. Already at the beginning of the reaction, the derivatives of α -TCP dissolution and CDHA formation are both remarkably higher in the reference, which indicates that the reaction is impeded from the

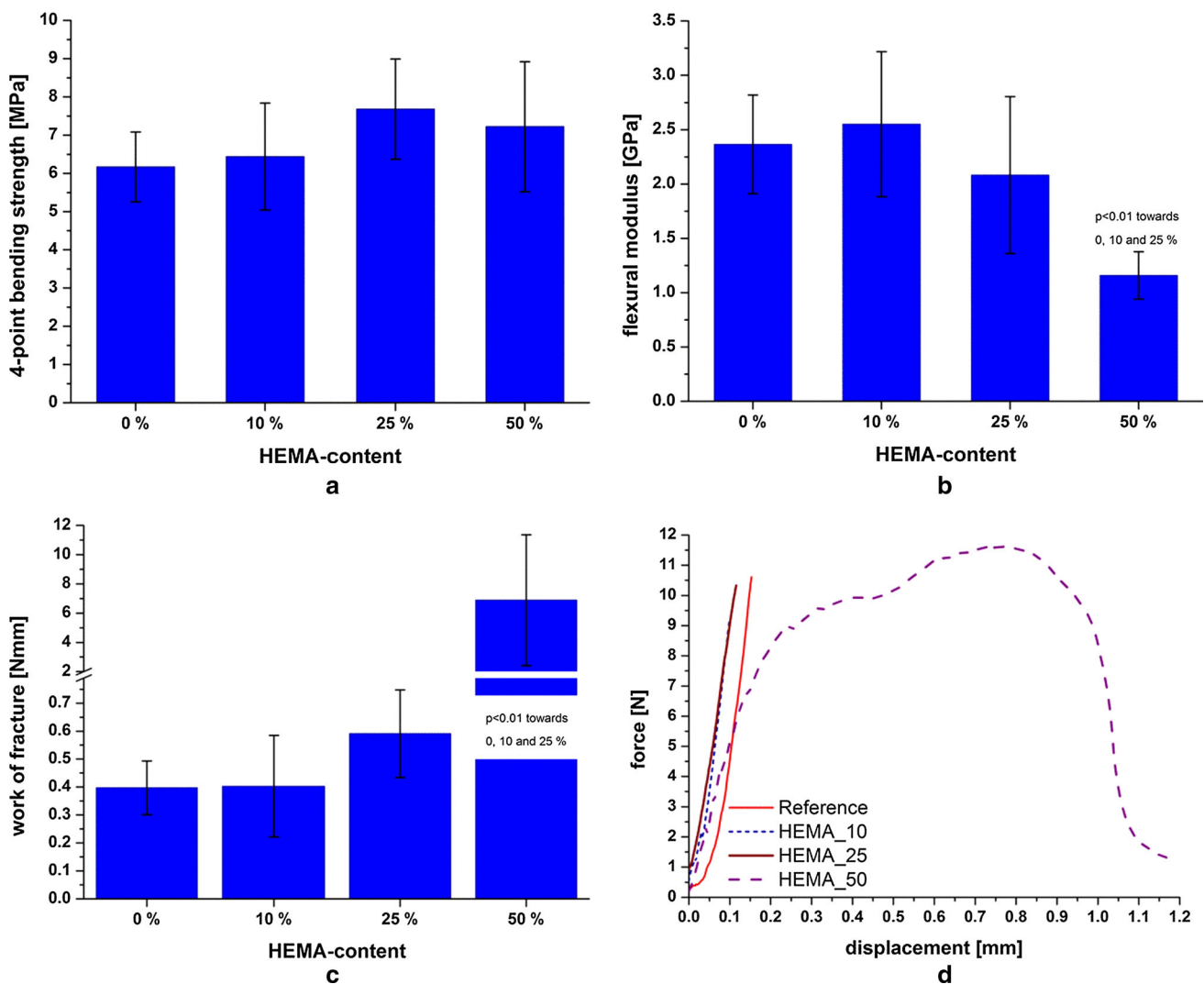


Fig. 4 Four-point-bending strength (a), flexural modulus (b), work of fracture (c) and force displacement curves (d) of samples with a geometry of $3 \times 4 \times 45$ mm. The samples were made of α -TCP and

a 2.5 % Na_2HPO_4 solution (reference) or of α -TCP and 10, 25 or 50 % HEMA solution (HEMA_10, HEMA_25 or HEMA_50) with a LPR of 0.33 ml/g and stored for 2 days in water at 37 °C

beginning. After 48 h of hydration, 9.1 ± 0.6 wt% α -TCP and 54.1 ± 2.4 wt% CDHA were present in the reference, while a composition of 24.6 ± 3.7 wt% α -TCP and 34.0 ± 1.8 wt% CDHA was obtained in HEMA_50.

Comparison of the quantitative phase content after 48 h of hydration in samples containing 0, 10, 25 and 50 wt% HEMA displayed a continuously increasing α -TCP content and decreasing CDHA content with increasing HEMA content of the cement liquid (Fig. 8).

XRD of the storage samples hydrated over 7 days showed that in both the reference and HEMA_50 an increase of CDHA content and correspondingly a decrease of α -TCP content was detected compared to the corresponding samples measured after 2 days. Even after 7 days, the CDHA content in the reference was considerably higher than in the α -TCP/HEMA composite (Fig. 9).

While in the reference 3.2 ± 0.4 wt% α -TCP and 61.3 ± 2.0 wt% CDHA were present, in HEMA_50 a composition of 20.3 ± 2.3 wt% α -TCP and 42.9 ± 4.5 wt% CDHA was obtained.

3.4 XRD crystallite sizes of CDHA

The determined mean coherent scattering domain (CSD) sizes from TOPAS were used for the crystallite sizes of CDHA. In directions of both the crystallographic a axis and the crystallographic c axis crystallite sizes were higher in the reference, compared to the α -TCP/HEMA composites (Fig. 10). The differences were not large, but significant. Indeed, no significant differences between the samples with different HEMA contents except 0 wt% HEMA were observed.

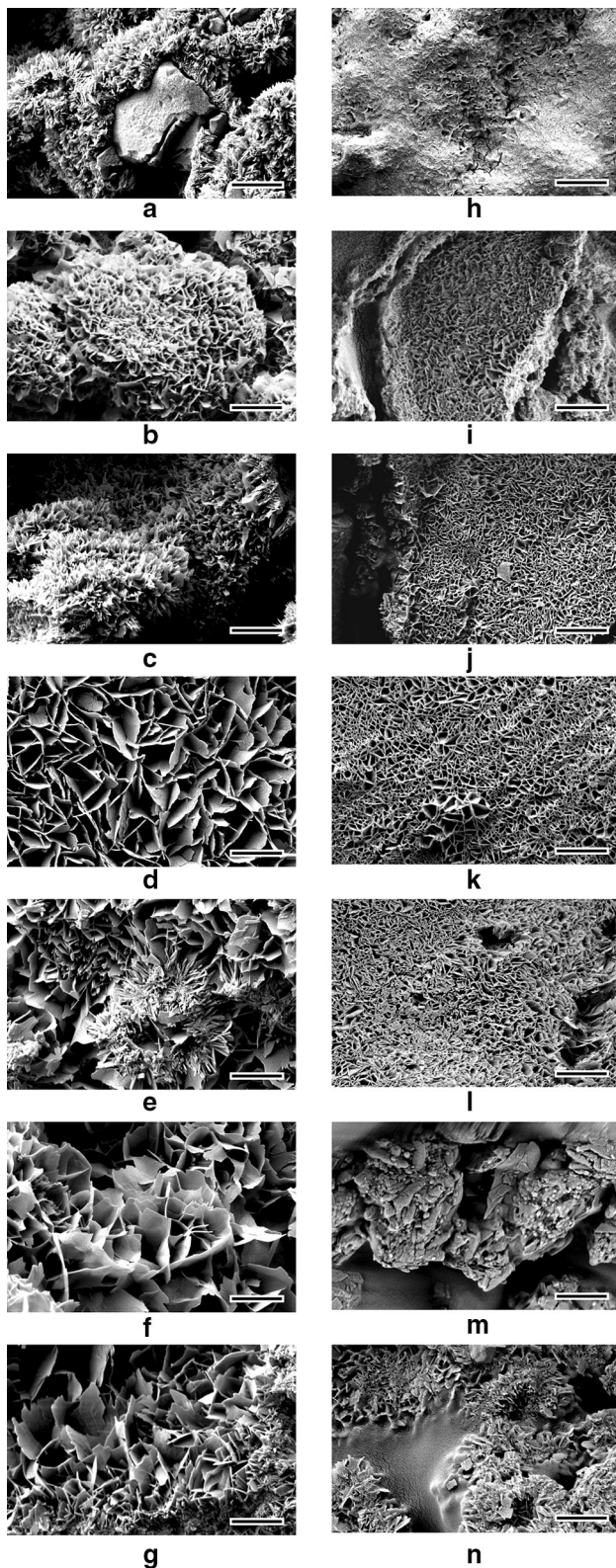


Fig. 5 Scanning electron micrographs of fracture surfaces with a 20,000 fold magnification. The samples were made of α -TCP and a 2.5 % Na_2HPO_4 solution (a–g) or of α -TCP and 50 % HEMA solution (h–n) with a LPR of 0.33 ml/g and stored for 2 h (a, h), 4 h (b, i), 6 h (c, j), 12 h (d, k), 24 h (e, l), 2 days (f, m) or 7 days (g, n) in water at 37 °C. The scale bar of all micrographs is 1 μm

The aspect ratio r_z/r_x , which describes the elongation of the hexagonal CDHA crystallites, was not significantly affected by varying the HEMA content. As the aspect ratio was about 3.5 in all samples, the hexagonal CDHA crystallites were clearly elongated in the direction of the crystallographic c axis.

4 Discussion

4.1 Influence of HEMA on α -TCP hydration

Modification of α -TCP with addition of HEMA previously has been demonstrated to be a promising method to improve the mechanical performance of α -TCP cements without affecting other cement properties like injectability [11]. Hence, in the present study more detailed investigations were performed to obtain further relevant information for a successful clinical application of such dual-setting cements. One important point is the influence of the polymeric phase on the hydration kinetics of α -TCP. Therefore quantitative in situ XRD measurements, including necessary corrections concerning the water loss inevitably occurring during these measurements, were accomplished. While the general effect of HEMA reducing the amount of α -TCP conversion to CDHA was previously observed by Christel et al. [11], this study supplied additional time-dependent quantitative data providing information about hydration kinetics.

It was shown by comparing the development of quantitative phase content in hydrating α -TCP powders with addition of 0 respectively 50 wt% HEMA in the mixing liquid that hydration of α -TCP to CDHA was considerably impeded by HEMA (Fig. 7). The time when maximum α -TCP dissolution occurred was only slightly shifted by HEMA, though the height of the maximum and the amount of dissolved α -TCP was strongly reduced. This indicates that the general reaction kinetics of α -TCP hydration are not changed by HEMA addition, while the overall extent of the reaction is reduced.

Comparison of the quantitative phase composition after 48 h in samples with HEMA contents of 0, 10, 25 and 50 wt% in the cement liquid demonstrated that different HEMA concentrations actually affect the hydration to a different extend (Fig. 8). This observation was generally

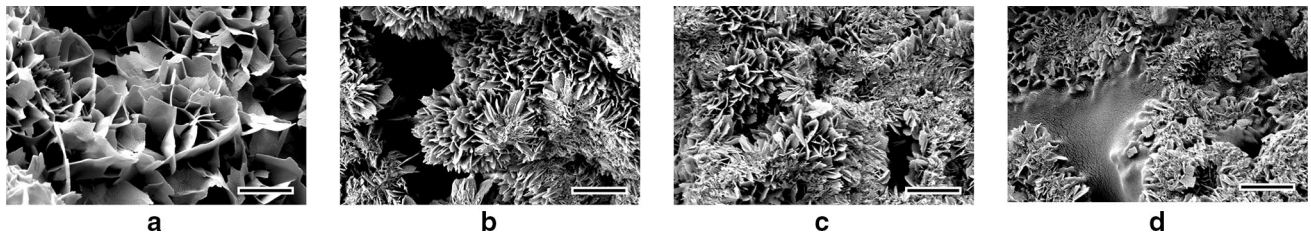


Fig. 6 Scanning electron micrographs of fracture surfaces with a 20,000 fold magnification. The samples were made of α -TCP and an aqueous solution containing 0 % (a), 10 % (b), 25 % (c) or 50 %

(d) of HEMA with a LPR of 0.33 ml/g. The samples were stored for 2 days in water at 37 °C. The scale bar of all micrographs is 1 μ m

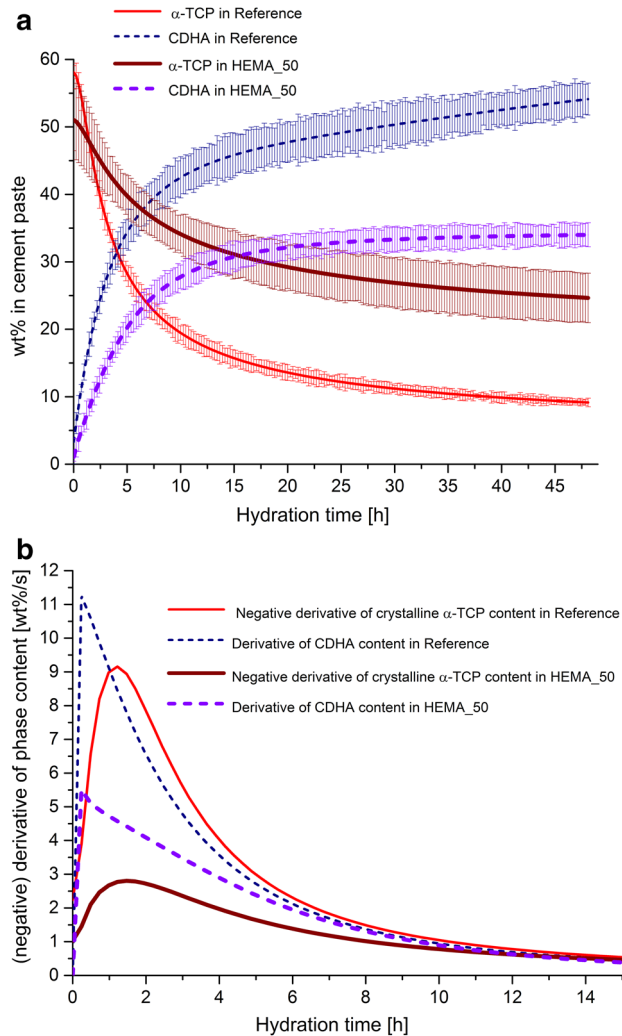


Fig. 7 Development of quantitative phase content of samples during hydration, determined by in situ XRD with subsequent Rietveld refinement and G-factor method (a), and derivatives of the phase content development (b). The samples were made of α -TCP and a 2.5 % Na_2HPO_4 solution (0 %) or 50 % HEMA solution with a LPR of 0.33 ml/g. Measurements were performed at 37 °C

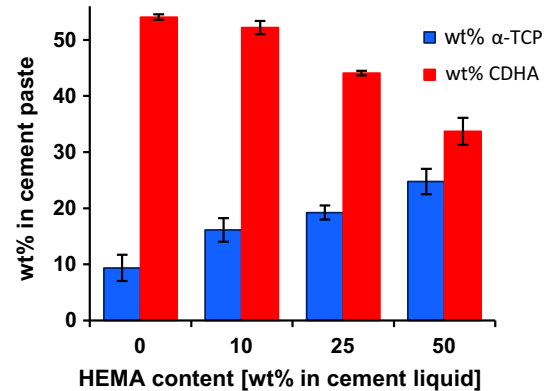


Fig. 8 Quantitative phase composition of samples after 48 h of hydration, determined by in situ XRD with subsequent Rietveld refinement and G-factor method. The samples were made of α -TCP and a 2.5 % Na_2HPO_4 solution (0 %) or of α -TCP and 10, 25 or 50 % HEMA solution with a LPR of 0.33 ml/g and stored for 2 days in closed plastic cups in a drying oven at 37 °C

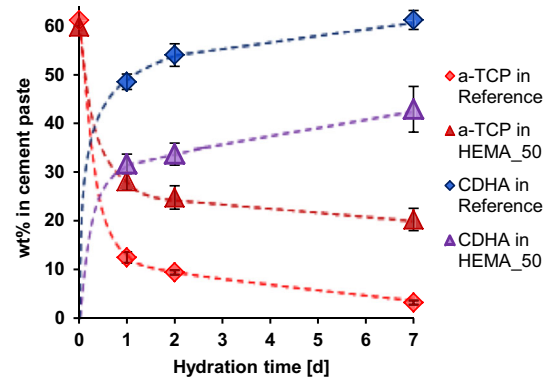


Fig. 9 Quantitative phase composition of samples, determined by in situ XRD with subsequent Rietveld refinement and G-factor method. The samples were made of α -TCP and a 2.5 % Na_2HPO_4 solution (0 %) or of α -TCP and 10, 25 or 50 % HEMA solution with a LPR of 0.33 ml/g and stored for 2 days in closed plastic cups in a drying oven at 37 °C

made already in [11], while in the present study samples with lower HEMA content (10 and 25 wt%) were additionally investigated and absolute quantitative data

obtained by G-factor method were provided. It was shown here that already 10 wt% HEMA addition led to a noticeable reduced hydration of α -TCP.

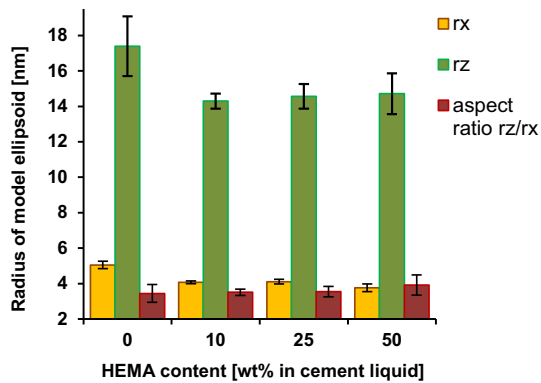


Fig. 10 Crystallite sizes of CDHA in direction of the crystallographic a axis (rx) and the crystallographic c axis (rz) in samples after 48 h of hydration, determined by in situ XRD using a model of Ectors et al. [17]. The samples were made of α -TCP and a 2.5 % Na_2HPO_4 solution (0 %) or of α -TCP and 10, 25 or 50 % HEMA solution with a LPR of 0.33 ml/g and stored for 2 days in closed plastic cups in a drying oven at 37 °C

Even after hydration over 7 days significantly more CDHA was formed in the reference sample, compared to samples containing 50 wt% HEMA (Fig. 9). It follows that HEMA not only retards the hydration, but generally reduces the amount of CDHA that can be formed in the samples. This indicates that the water absorbed by the p-HEMA hydrogel during polymerisation permanently remains unavailable for α -TCP hydration. It also has to be considered that the amount of water actually present in the cement paste is lower in HEMA_50, as 1 ml of cement liquid was used in each case and parts of the water in the cement liquid were replaced by the HEMA monomer. Water content of the cement pastes was reduced from 24.4 wt% in the reference to 12.8 wt% in HEMA_50, which diminishes the amount of water available for hydration.

Additionally water is physically bound in the hydrogel forming during polymerisation of HEMA. Hence it is most likely that the reduction of the amount of free water actually available for the hydration of α -TCP is responsible for reduction of the reaction rate. If less water is available in the cement paste, less α -TCP can be dissolved. As was clearly shown by time-dependent in situ XRD measurements, the reducing effect of HEMA on the reaction rate was observed directly since the beginning of hydration. Another aspect which is expected to affect the hydration is a reduction of the diffusion speed of both calcium and phosphate ions due to reduced H_2O as a result of hydrogel formation, which retards CDHA crystal growth. This might also explain the fact that HEMA was shown to decrease CDHA crystal sizes visible in SEM images.

Hydration might also be physically impeded by the HEMA polymer. During setting of HEMA modified α -TCP

cements, HEMA and CDHA form two interpenetrating matrices [11]. The HEMA polymer, which is present in the form of poly-HEMA-chains in the hardened samples, might complicate further dissolution of the α -TCP grains. This would also explain that the effect is stronger for higher HEMA concentrations, where more polymer volume is present.

Nevertheless, this study also clearly demonstrated that despite the impeding effect of HEMA, the hydration of α -TCP was not completely stopped. Although the amount of CDHA formed during hydration was considerably reduced, even with addition of 50 wt% HEMA to the cement liquid a considerable amount of CDHA could be formed and after about 15 h the amount of quantified CDHA exceeded that of residual α -TCP (Fig. 7a). It is also interesting that the maximum of CDHA formation is located rather early with addition of 50 wt% HEMA. This means that despite the strong overall reduction of the hydration reaction at least a considerable amount of CDHA forms rather quickly.

The α -TCP and CDHA quantities measured in this study were compared with the corresponding quantities obtained in Christel et al. [11] for the samples where the same HEMA concentrations were used. Degree of conversion was about 80 % after 1 day and about 95 % after 7 days for the reference in this study. This is in good agreement with the data from [11], where degrees of conversion of 82 ± 2 % (1 day) and 96 ± 1 % (7 days) were obtained. For HEMA_50, degrees of conversion of 55 % (1 day) and 81 % (7 days) measured in [11] are compared to 54 ± 4 % (1 day) and 68 ± 5 % (7 days) in the present study. The data were nearly identical after 1 day.

Except for the α -TCP/HEMA composite after 7 days, where a noticeable difference of 13 % occurred, the values obtained in both studies are very good in agreement. The difference in that sample could be due to the different experimental conditions. The samples in [11] were stored in a water bath, while in the present study they were hardened in sealed crucibles. The availability of water (which is physically bound in the poly-HEMA hydrogel in a considerable amount) was therefore presumably still higher in [11], which might lead to a higher conversion rate there. Nevertheless, as the difference even after 7 days is not enormous, it can be concluded that the reaction is not extremely sensible to slight modifications in the experimental environment, as long as the temperature is identical and water loss is impeded.

4.2 Visible crystal sizes and XRD mean crystallite sizes of CDHA

The apparent size of CDHA crystals visible under SEM decreased with increasing HEMA content (Fig. 6), while the crystallite sizes determined from Rietveld refinement

were indeed generally reduced by HEMA addition, but did not show any correlation with the HEMA content of the sample (Fig. 10). In the Rietveld refinement procedure the sizes of coherent scattering domains (CSD) in CDHA are determined as crystallite sizes, which do not necessarily correspond to the size of the CDHA crystals visible under the microscope—these crystals might be mosaic crystals consisting of several crystallites, with the result that the visible crystals can be larger than the XRD crystallite sizes (Fig. 11).

The morphology of the CDHA crystals, which were detected in SEM images of the reference sample, did not directly correspond to the crystallite morphology determined by XRD, which were shown to be clearly elongated in the direction of the crystallographic *c* axis. This indicates that the visible CDHA crystals are actually mosaic crystals, which is also confirmed by the fact that the size of visible crystallites strongly exceeds the XRD crystallite size. The CDHA crystallites determined in this study show the general anisotropy that was previously described for CDHA forming in α -TCP cements [20] and was also observed in natural bone [21]. This general observation was obviously not changed by addition of HEMA.

The mean crystallite size of CDHA has to be taken into account for evaluation of the biological performance of the material. Reduced mean crystallite size is expected to have a positive effect on bone formation, since increased bone formation for CDHA with lower XRD crystallite size measured by XRD using the Scherrer and Hall method was observed for composite scaffolds containing CDHA [22].

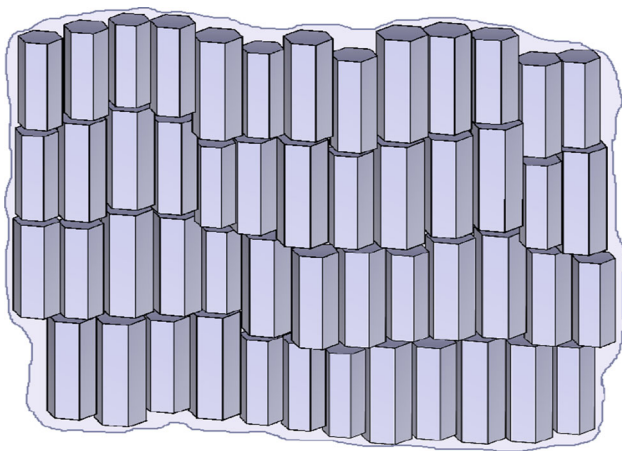


Fig. 11 Schematic model of a part of a CDHA mosaic crystal consisting of several separate coherent scattering domains (CSD), which are elongated in direction of the crystallographic *c* axis; the models for the CSD's were created with VESTA [23]

4.3 Mechanical performance and relation to CDHA formation

The mechanical performance of 2 days hardened TCP cements could be improved by modifying them with HEMA. Addition of 50 wt% HEMA to the cement liquid changed the brittle performance of the hardened cement to a pseudoplastic behaviour, reduced the flexural modulus and highly increased the work of fracture, while lower HEMA concentrations had no comparable effect (Fig. 4). Consequently a minimum content of the ductile polymer is required to overcome the brittleness of hardened α -TCP cements, while for lower HEMA concentrations the brittle CDHA ceramic still determines the mechanical performance. It was already observed in [11] that samples with 50 % HEMA or more were significantly more flexible, while lower concentrations did not have a noticeable effect. Work of fracture was increased by an order of magnitude with addition of 50 wt% HEMA, compared to the reference sample, and still four times higher than what was achieved with addition of 40 wt% HEMA [11]. Therefore 50 wt% actually is the critical HEMA content to change the mechanical performance in the desired way.

In this study, additionally the time dependent strength development was investigated, which is important to evaluate the performance of the cement in the first time after application. Furthermore, the time dependent measurements allowed the correlation of mechanical properties with the development of quantitative phase content.

The strength development of the α -TCP samples with and without HEMA modification was compared with the setting reaction of α -TCP, described by the development of the quantitative α -TCP and CDHA content. While the maximum of CDHA formation rate was already observed after about 1 h, significant increase in bending strength was only measured between 6 and 12 h in both the reference and HEMA_50. In the time between 6 and 12 h the CDHA content increased from 37 ± 3 to 44 ± 3 wt% in the reference and from 23 ± 2 to 29 ± 2 wt% in HEMA_50. Hence the data suggest that the initial rapid CDHA formation does not really contribute to the measured bending strength. As this accounted for both the reference and HEMA_50, the increase of bending strength during this time can only result from the slight increase in amount of CDHA or from a change in CDHA network. This is also supported by the measurements after 2 days showing that bending strength is not increasing with HEMA content in the cement liquid (Fig. 4). Bending strength therefore must be related to the inorganic part of the composite. Actually, SEM images of the hardened cement have shown that the size of visible CDHA crystals in the reference increased between 6 and 12 h (Fig. 5c, d), which might indicate that CDHA crystal growth and the formation of crystal mosaics

as mentioned above is responsible for the strong increase of the bending strength.

For the work of fracture, a significant increase between 6 and 12 h was observed in the reference sample, which is comparable to the increase in bending strength. As the work of fracture was very high in HEMA_50 even after 2 h and it did not change during hydration, it follows that the increased work of fracture mainly results from the HEMA polymer, which achieves its final work of fracture rather quickly due to the fast reaction and exceeds that of the reference by an order of magnitude.

All here determined mechanical parameters (four-point bending strength, flexural modulus and work of fracture) showed their main increase considerably later (2–6 h) than the major part of CDHA formation (1–2 h), whereas for pure β -TCP cements in [13] a linear relation between CDHA content and strength was observed. Nevertheless, in [13] only the compressive strength was determined, hence there is no contradiction between these data. Indeed, as a linear correlation between CDHA content and compressive strength was shown to exist in [13], it can in turn be concluded that the development of compressive strength follows the course of CDHA formation, which was provided in this study. It is also noteworthy that contrary to the other mechanical parameters the flexural modulus still significantly increased after 12 h in the reference sample. CDHA content during this time only increased from 44 ± 3 to 49 ± 3 wt%, which indicates that the increase in flexural modulus cannot be directly attributed to more CDHA formation.

5 Conclusions

In this study the influence of HEMA addition to the cement liquid on the setting kinetics of α -TCP was investigated, which is essential for successful clinical application of α -TCP/HEMA composites. The extent of CDHA formation was reduced by HEMA, while the general reaction kinetics were not changed. Addition of 50 wt% HEMA is sufficient to obtain a pseudoplastic behaviour of the hardened cements, reduce the flexural modulus and strongly increase work of fracture. Consequently, an α -TCP/HEMA composite fabricated with addition of 50 wt% HEMA to the cement liquid might be suitable for application in some load bearing defects due to its improved mechanical properties, especially if additional approaches for further optimization like addition of cross-linkers to the polymer are applied.

As CDHA formation was shown to be rather rapid at the beginning of hydration in both the reference and HEMA_50, it follows that compressive strength is expected to develop rather quickly in the hardening cement

pastes. Work of fracture was shown to be high from the beginning in sample HEMA_50, hence the composite develops its ability to withstand mechanical stress rather early. Due to the improved mechanical properties, mechanical treatment of hardening cement pastes shortly after implementation e.g. by drilling and implementation of screws should be possible using the α -TCP/HEMA composite.

We conclude that the lower flexural modulus cannot be attributed to CDHA formation but to the formed HEMA polymer. SEM images of the hardened cement have shown that the size of visible CDHA crystals increased between 6 and 12 h synchronous to the observed increase in bending strength. This CDHA crystal growth which is resulting in a network of overlapping platy crystals is responsible for the strong increase of the bending strength. Bending strength therefore must be related to the inorganic part of the composite.

The significantly lower CDHA formation in α -TCP/HEMA composites must be related to reduction of available H_2O : (a) by less H_2O in the cement liquid, (b) by creation of a HEMA network by polymerisation and inclusion of H_2O drops in its network and (c) by adsorption of H_2O at its surfaces. Less dissolution of α -TCP and precipitation of CDHA are the consequence.

Hence the α -TCP/HEMA composite might be further optimized by using more reactive α -TCP, for example α -TCP powders with high ATCP content.

References

1. Dorozhkin SV. Calcium orthophosphate cements for biomedical application. *J Mater Sci.* 2008;43(9):3028–57.
2. Gbureck U, Spatz K, Thull R, Barralet JE. Rheological enhancement of mechanically activated alpha-tricalcium phosphate cements. *J Biomed Mater Res Part B.* 2005;73B:1–6.
3. Canal C, Ginebra MP. Fibre-reinforced calcium phosphate cements: a review. *J Mech Behav Biomed Mater.* 2011;4:1658–71.
4. Moreau JL, Weir MD, Xu HHK. Self-setting collagen-calcium phosphate bone cement: mechanical and cellular properties. *J Biomed Mater Res A.* 2009;91A(2):605–13.
5. Schneiders W, Reinstorf A, Biewener A, Serra A, Grass R, Kinscher M, Heineck J, Rehberg S, Zwipp H, Rammelt S. In vivo effects of modification of hydroxyapatite/collagen composites with and without chondroitin sulphate on bone remodeling in the sheep tibia. *J Orthop Res.* 2009;27(1):15–21.
6. Wu TY, Zhou ZB, He ZW, Ren WP, Yu XW, Huang Y. Reinforcement of a new calcium phosphate cement with RGD-chitosan-fiber. *J Biomed Mater Res Part A.* 2014;102:68–75.
7. Xu HHK, Simon CG. Fast setting calcium phosphate-chitosan scaffold: mechanical properties and biocompatibility. *Biomaterials.* 2005;26:1337–48.
8. dos Santos LA, Carrodeguas RG, Boschi AO, de Arruda ACF. Fiber-enriched double-setting calcium phosphate bone cement. *J Biomed Mater Res Part A.* 2003;65A(2):244–50.

9. dos Santos LA, Carrodeguas RG, Boschi AO, de Arruda ACF. Dual-setting calcium phosphate cement modified with ammonium polyacrylate. *Artif Organs*. 2003;27(5):412–8.
10. Wang J, Liu CS, Liu YF, Zhang S. Double-network interpenetrating bone cement via in situ hybridization protocol. *Adv Funct Mater*. 2010;20(22):3997–4011.
11. Christel T, Kuhlmann M, Vorndran E, Groll J, Gbureck U. Dual setting alpha-tricalcium phosphate cements. *J Mater Sci Mater Med*. 2013;24(3):573–81.
12. Ginebra MP, Fernandez E, Driessens FCM, Planell JA. Modeling of the hydrolysis of α -tricalcium phosphate. *J Am Ceram Soc*. 1999;82(10):2808–12.
13. Gbureck U, Grolms O, Barralet JE, Grover LM, Thull R. Mechanical activation and cement formation of beta-tricalcium phosphate. *Biomaterials*. 2003;24:4123–31.
14. Jansen D, Stabler Ch, Goetz-Neunhoeffer F, Ditttrich S, Neubauer J. Does Ordinary Portland Cement contain amorphous phase? A quantitative study using an external standard method. *Powder Diffr*. 2011;26:31–8.
15. Mathew M, Schroeder LW, Dickens B, Brown WE. The crystal structure of α -Ca₃(PO₄)₂. *Acta Crystallogr B*. 1977;33:1325–33.
16. Sudarsanan K, Young RA. Significant precision in crystal structural details: Holly Springs hydroxyapatite. *Acta Crystallogr Sect B*. 1969;25:1534–43.
17. Ectors D, Goetz-Neunhoeffer F, Neubauer J. A generalized geometric approach to anisotropic peak broadening due to domain morphology. *J Appl Crystallogr*. 2015;48:189–94.
18. International Union for Crystallography, Prince E. *International Tables for Crystallography, Volume C. Mathematical Physical and Chemical Tables*. 3rd ed. New York: Wiley; 2004.
19. Wojdyr M. Fityk: a general-purpose peak fitting program. *J Appl Crystallogr*. 2010;43:1126–8.
20. Hurler K, Neubauer J, Bohner M, Doebelin N, Goetz-Neunhoeffer F. Effect of amorphous phases during the hydraulic conversion of α -TCP into calcium deficient hydroxyapatite. *Acta Biomater*. 2014;10(9):3931–41.
21. Psycharis V, Kalamakis N, Boukos N, Trapalis C, Bourlino A, Karakasides M. Chemical and X-ray diffraction peak broadening analysis, electron microscopy and ir studies of biological apatites. *Mater Sci Forum*. 2001;378–381:759–64.
22. Hayakawa T, Mochizuki C, Hara H, Fukushima T, Yang F, Shen H, Wang S, Sato M. Influence of apatite crystallinity in porous PLGA/apatite composite scaffold on cortical bone response. *J Hard Tissue Biol*. 2009;18(1):7–12.
23. Momma K, Izumi F. VESTA 3 for three-dimensional visualization of crystal, volumetric and morphology data. *J Appl Crystallogr*. 2011;44:1272–6.